

Supporting Information

Amplified Spontaneous Emission in Insulated Polythiophenes

*Chen Sun^a, Marta M. Mroz^a, José Raúl Castro Smirnov^a, Larry Lüer^a, Chunhui Zhao^b, Masayuki Takeuchi^b, Kazunori Sugiyasu^b, and Juan Cabanillas- González^{*a}*

^aMadrid Institute for Advanced Studies (IMDEA Nanociencia), Ciudad Universitaria de Cantoblanco, Calle Faraday 9, Madrid 28049, Spain

^bMolecular Design & Function Group, National Institute for Materials Science (NIMS), 1-2-1 Sengen, Tsukuba, Ibaraki 305-0047, Japan.

*Email - juan.cabanillas@imdea.org

Material and device preparation

Regioregular poly(3-hexylthiophene) (RR-P3HT) was purchased from commercial suppliers and used without further purification. (BASF Sepiolid P200, > 98% regioregularity, $M_n \sim 20\text{-}30$ kg/mol). The red emitting supramolecular isolated $\frac{1}{2}$ IPT and IPT (chemical structure shown in Scheme 1) consists of a polythiophenes backbone with cyclic side chains, the synthesis method is described elsewhere¹⁷ and $\frac{1}{2}$ IPT is described below. Diluted RR-P3HT, $\frac{1}{2}$ IPT and IPT solutions were prepared from chloroform: 0.1 mg/mL for P3HT and $\frac{1}{2}$ IPT solution and 0.25 mg/mL for IPT to keep the absorption values approximately the same at 387.5 nm. A chloroform solution of P3HT, $\frac{1}{2}$ IPT and IPT (10 mg/ml) was stirred overnight to form a homogeneous solution. Thereafter, the three materials were spin-coated at 1500 r/min for 30 s onto the quartz substrates to form condensed films. The thickness of the prepared thin film was estimated to be 75, 160 and 210 nm for P3HT, $\frac{1}{2}$ IPT and IPT respectively.

Steady state experiments.

All spectra were taken at room temperature in ambient conditions. UV-Visible absorption spectra were recorded using Varian Cary 500 UV-Vis spectrophotometer, while the photoluminescence spectra were recorded using a spectrofluorometer from HORIBA Scientific. The photoluminescence quantum efficiency (PLQE) of the polymers was measured using an Edinburgh FLSP920 fluorescence spectrophotometer equipped with a Xenon arc lamp (Xe900) using an integrating sphere. Background corrected Raman spectra were recorded exciting at 532 nm (20x objective, 5 mW excitation power) with a Senterra (Bruker) Raman microscope and averaging four consecutive measurements on different positions on the sample, (5s acquisition time for each spectra).

ASE experiments

The samples were optically pumped at 387.5 nm with the second harmonic of a femtosecond regenerative amplifier (Clark-MXR model CPA-1) delivering pulses of 150 fs duration at 1 kHz repetition rate. A cylindrical lens combined with a slit was used to create a narrow excitation stripe of $110\ \mu\text{m} \times 3\ \text{mm}$. In order to optimize the measurements, the laser stripe was positioned on the sample parallel to the substrate edges. The photoluminescence arising from the edge of the waveguide was spectrally dispersed with a spectrometer (SP2500, Acton Research) equipped with a liquid nitrogen cooled back-illuminated deep depletion CCD (Spec-10:400BR, Princeton Instruments). The pumping intensity was regulated with neutral density filters. The threshold values were obtained from the dependence of the emission integrated intensity and FWHM on the input fluence.

TA experiments

Pump-probe measurements were carried out with a Clark-MXR model CPA-1 regenerative amplifier, which delivers pulses at 775 nm (1 kHz, 150 fs, 500 μ J). The primary beam was split into pump and probe beams. The pump pulse was generated by a BBO crystal for second harmonic generation (387.5 nm) and attenuated to reach an excitation density of 6.8×10^{-2} mJ/cm². Broadband supercontinuum pulses were generated by focusing a portion of the fundamental onto a sapphire plate (1 mm thick) and the delay line was controlled by a computer to anticipate it respect to the probe. Both pulses were temporally and spatially overlap on the sample. After transmission through the sample, the probe pulses and a reference probe were sent to a prism spectrometer (Entwicklungsburo Stresing GmbH) with a CCD array.

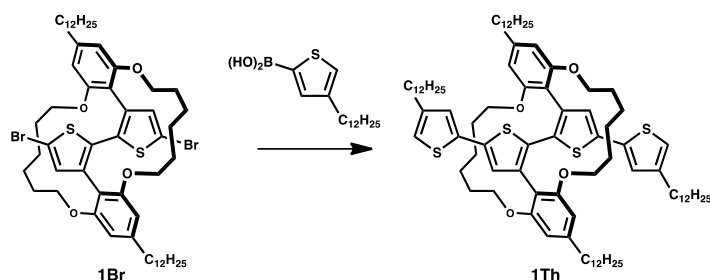
GIWAXS experiments

WAXS experiments have been conducted at the Dutch-Belgian Beamline (DUBBLE) station BM26B of the European Synchrotron Radiation Facility (ESRF) in Grenoble (France).

General

Nuclear magnetic resonance (NMR) spectra were recorded on a JEOL ECS-400 (400 MHz) spectrometer. All chemical shifts are reported in parts per million (ppm) from tetramethylsilane (0 ppm for ¹H) or residual CHCl₃ (77 ppm for ¹³C) as an internal standard. Matrix-assisted laser desorption ionization time-of-flight (MALDI-TOF) mass spectra were obtained using a Shimadzu Axima-CFR plus station. Synthesis of dibrominated monomer (**1Br**) has been reported previously.^{S1} From **1Br**, half insulated polythiophene $\frac{1}{2}$ **1PT** was synthesized as described below.

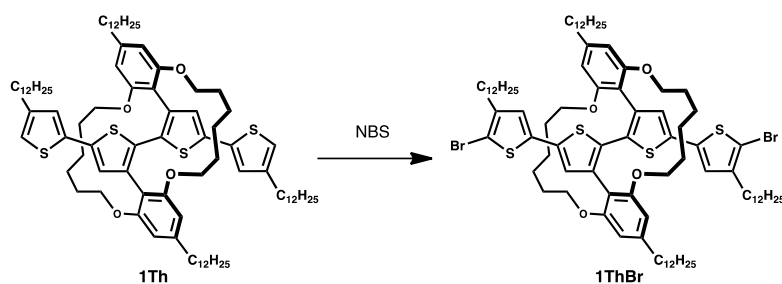
Synthesis of 1Th.



Under Ar atmosphere, to a solution of **1Br** (300 mg, 0.29 mmol), 4-dodecyl-2-thienylboronic acid (256 mg, 0.86 mmol) in a mixture of toluene (4 mL), ethanol (1 mL), and water (1 mL), tetrakis(triphenylphosphine)palladium(0) (16.6 mg, 0.014 mmol) was added, and the reaction mixture was stirred at 80 °C overnight. The mixture was cooled down to room temperature, washed with water, and dried over magnesium sulfate. Filtrate was concentrated, and the solid residue was purified through column chromatography (silica gel, hexane : dichloromethane = 3 : 1) to give **1Th** as a yellow powder (193 mg, yield: 48%). ¹H NMR (400 MHz, CDCl₃, 298 K) δ 0.87 (12H, m), 0.98 (4H, m), 1.27-1.58 (88H, m), 1.74 (4H, m), 2.52 (4H, t, J = 7.8 Hz), 2.68 (4H, t, J = 7.4 Hz), 3.75 (4H, m), 4.06 (4H, m), 6.53 (4H, s), 6.67 (2H, d, J = 1.2 Hz), 6.74 (2H, d, J = 1.2 Hz), 6.87 (2H, s). ¹³C NMR (150 MHz, CDCl₃, 298 K) δ 14.13, 22.70, 27.40, 29.38, 29.41, 29.56, 29.66, 29.71, 29.77, 30.31, 30.52, 31.92, 32.05, 36.80, 69.64, 107.23, 113.76,

117.91, 123.55, 126.07, 132.03, 132.36, 133.97, 138.01, 143.79, 146.15, 158.47. MALDI-TOF mass (dithranol): calcd. for $C_{88}H_{134}O_4S_4$ $[M]^+$: $m/z = 1383.92$; found: 1383.94.

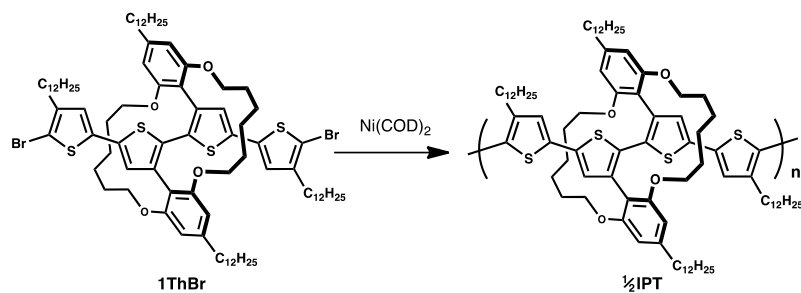
Synthesis of 1ThBr.



To a solution of **1Th** (120 mg, 0.087 mmol) in chloroform (10 mL) and acetic acid (1 mL) at 0 °C, *N*-bromosuccinimide (32.4 mg, 0.18 mmol) was added. The reaction mixture was stirred for 2 hours, washed with water, and dried over magnesium sulfate. Filtrate was concentrated, and the solid residue was purified through column chromatography (silica gel, hexane : dichloromethane = 3 : 1) to give **1ThBr** as a yellow powder (123 mg, yield: 92%). ¹H NMR (400 MHz, CDCl₃, 298 K) δ 0.87 (12H, m), 0.97 (4H, m), 1.27-1.51 (88H, m), 1.74 (4H, m), 2.47 (4H, t, $J = 7.8$ Hz), 2.63 (4H, t, $J = 7.8$ Hz), 3.74 (4H, m), 4.07 (4H, m), 6.53 (4H, s), 6.61 (2H, s), 6.83 (2H, s). ¹³C NMR (150 MHz, CDCl₃, 298 K) δ 14.14, 22.70, 27.45, 29.30, 29.38, 29.40, 29.43, 29.47, 29.52, 29.56, 29.65, 29.71, 29.76, 30.10, 30.29, 31.94, 32.05, 36.81, 69.65, 106.60, 107.17, 113.32, 122.92, 126.14, 132.42, 132.59, 133.20, 142.63, 146.30, 146.45, 158.42.

MALDI-TOF mass (dithranol): calcd. for $C_{88}H_{132}Br_2O_4S_4$ $[M+H]^+$: $m/z = 1541.74$; found: 1541.47.

Synthesis of $\frac{1}{2}$ IPT.



$\frac{1}{2}$ IPT was synthesized, through Yamamoto reductive polymerization using bis(1,5-cyclooctadiene)nickel(0), and purified in a similar manner as the case of IPT.^{S1} $M_n = 54.6K$, $M_w = 194.3K$, $M_w/M_n = 3.56$ (vs. polystyrene standard). 1H NMR (400 MHz, $CDCl_3$, 298 K) δ 0.87 (12H, t, $J = 6.8$ Hz), 1.01 (4H, br), 1.25-1.56 (88H, m), 1.72 (4H, br), 2.44 (4H, br), 2.68 (4H, br), 3.77 (4H, br), 4.08 (4H, br), 6.53 (4H, s), 6.74 (2H, br), 6.88 (2H, br). ^{13}C NMR (150 MHz, $CDCl_3$, 298 K) δ 14.14, 22.71, 27.45, 29.11, 29.41, 29.72, 29.76, 30.37, 30.80, 31.95, 36.72, 69.66, 107.14, 113.59, 123.68, 126.30, 126.65, 132.30, 132.54, 133.66, 137.86, 142.76, 146.19, 158.45.

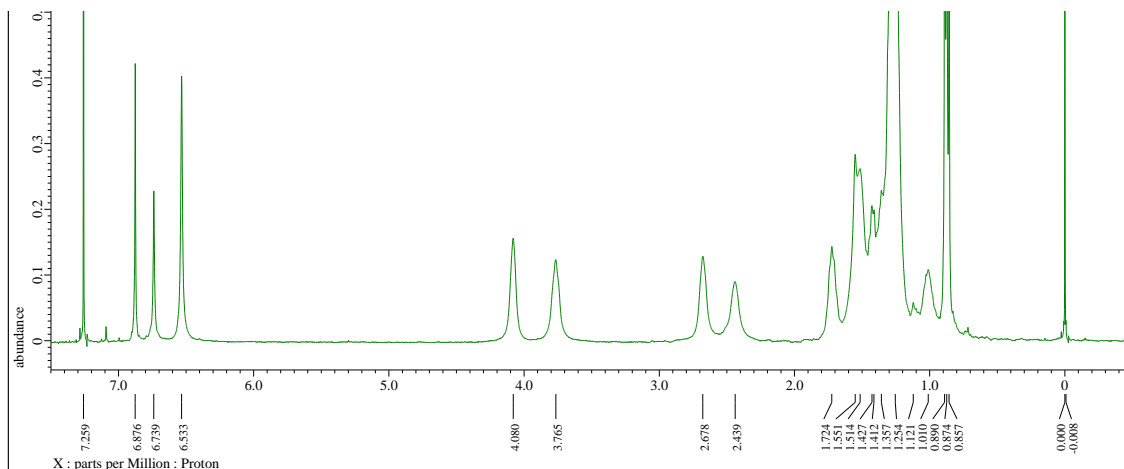


Fig. S1. ^1H NMR spectrum of $\frac{1}{2}\text{IPT}$.

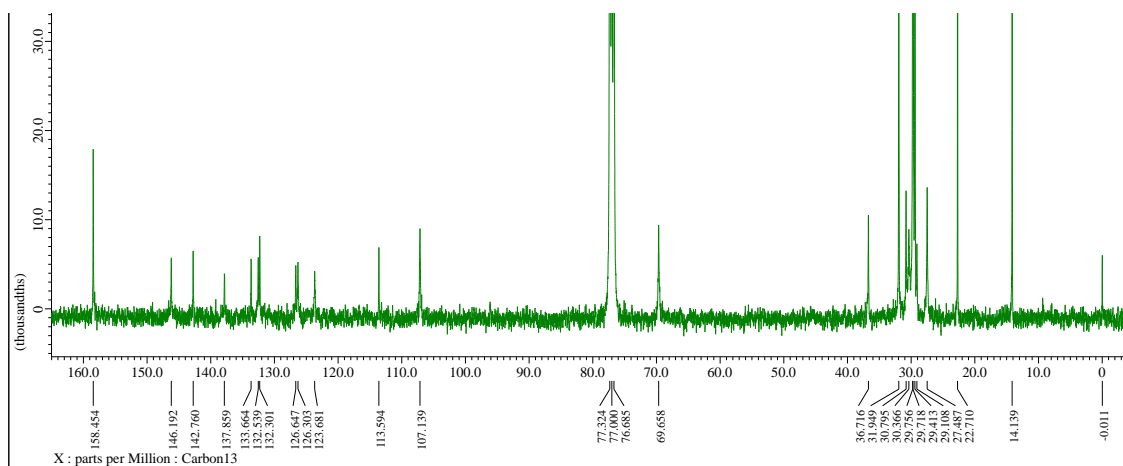


Fig. S2. ^{13}C NMR spectrum of $\frac{1}{2}\text{IPT}$.

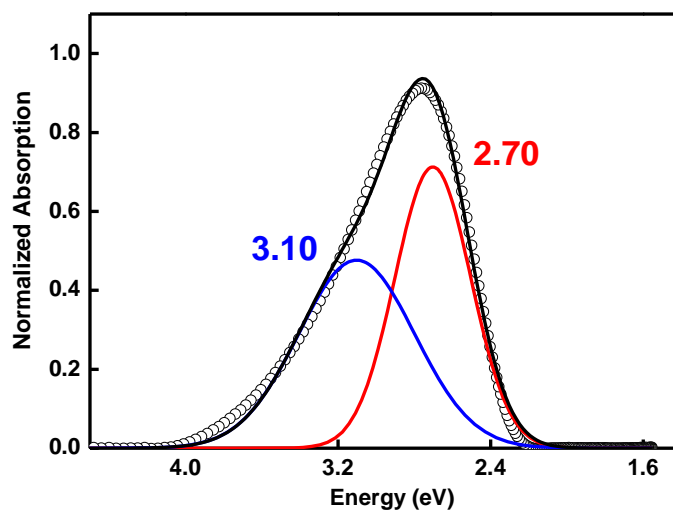


Fig. S3. UV spectra of P3HT in diluted chloroform solution (open circle) and straight lines stand for Gaussian fit.

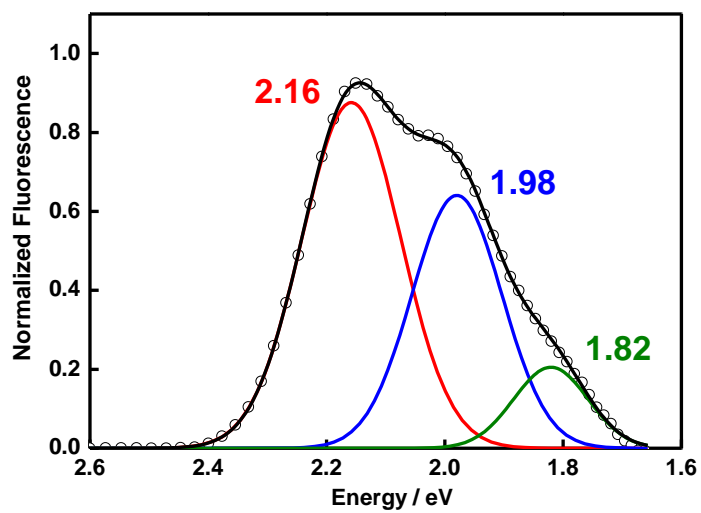


Fig. S4. PL spectra of P3HT in diluted chloroform solution (open circle) and straight lines stand for Gaussian fit.

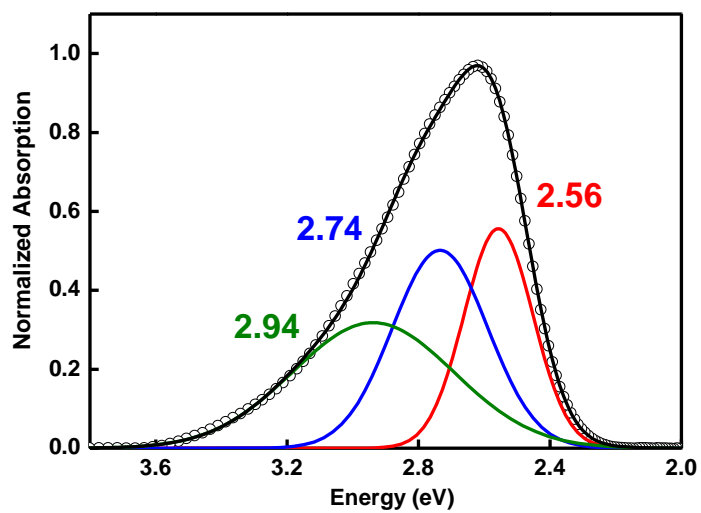


Fig. S5. UV spectra of $\frac{1}{2}$ IPT in diluted chloroform solution (open circle) and straight lines stand for Gaussian fit.

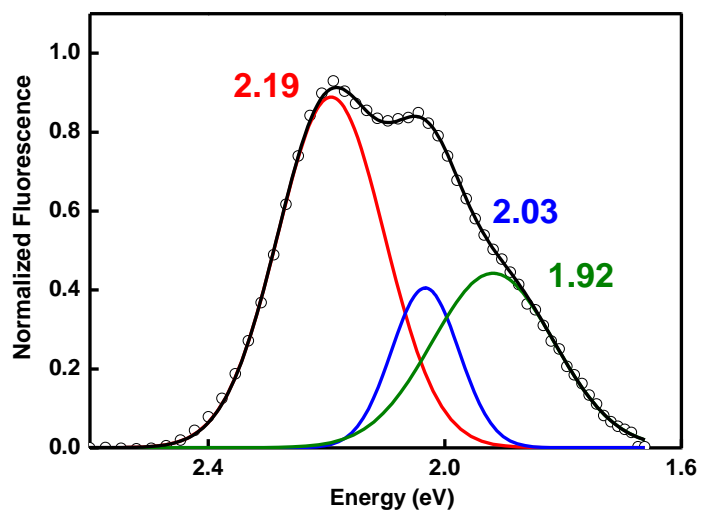


Fig. S6. PL spectra of $\frac{1}{2}$ IPT in diluted chloroform solution (open circle) and straight lines stand for Gaussian fit.

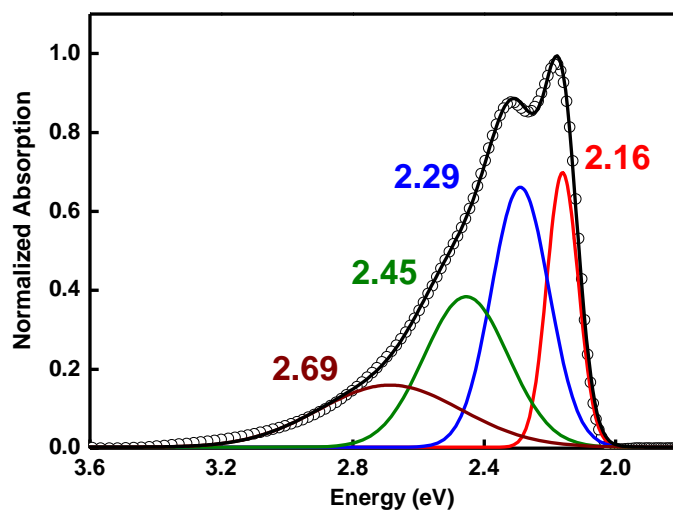


Fig. S7. UV spectra of IPT in diluted chloroform solution (open circle) and straight lines stand for Gaussian fit.

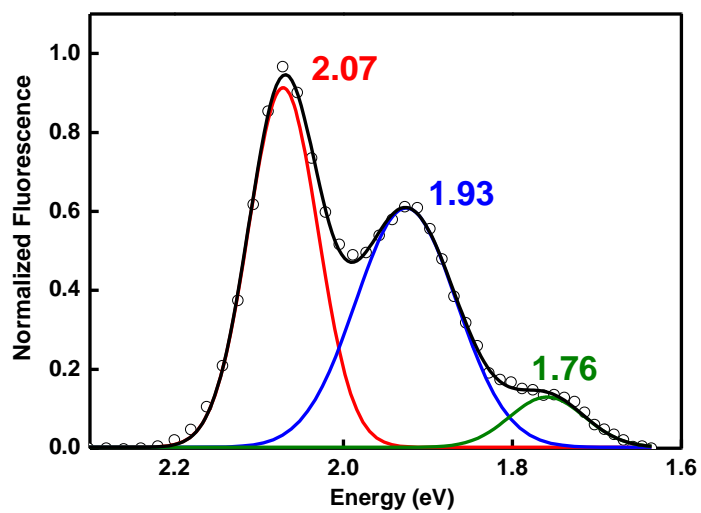


Fig. S8. PL spectra of IPT in diluted chloroform solution (open circle) and straight lines stand for Gaussian fit.

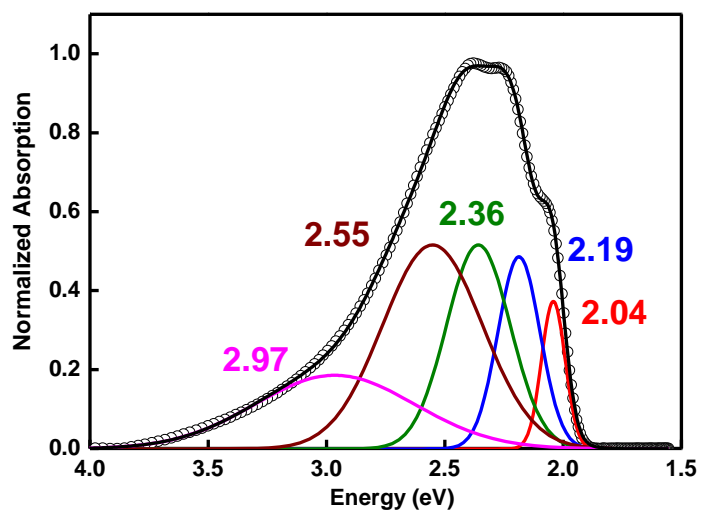


Fig. S9. UV spectra of P3HT in film spin-coated on quartz substrate (open circle) and straight lines stand for Gaussian fit.

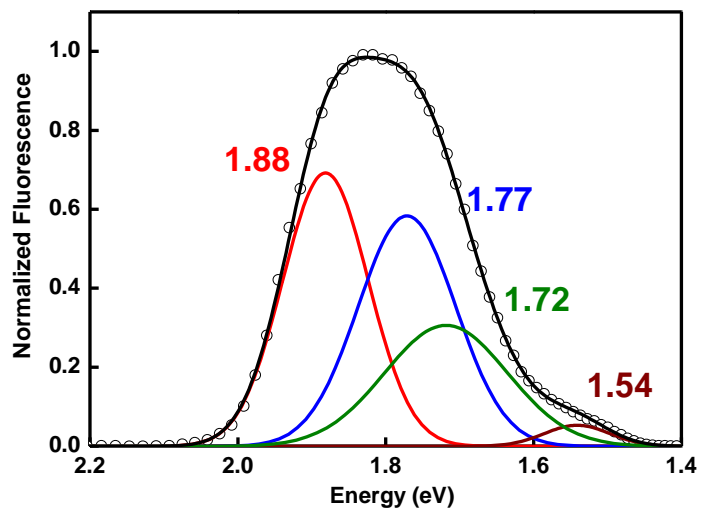


Fig. S10. PL spectra of P3HT in film spin-coated on quartz substrate (open circle) and straight lines stand for Gaussian fit.

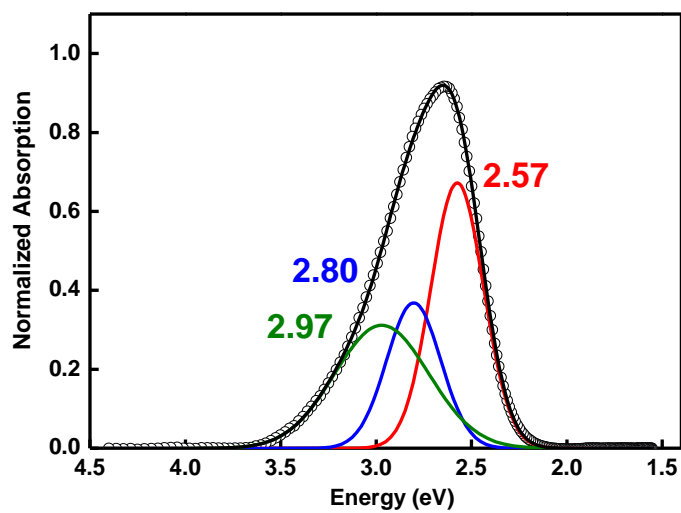


Fig. S11. UV spectra of $\frac{1}{2}$ IPT in film spin-coated on quartz substrate (open circle) and straight lines stand for Gaussian fit.

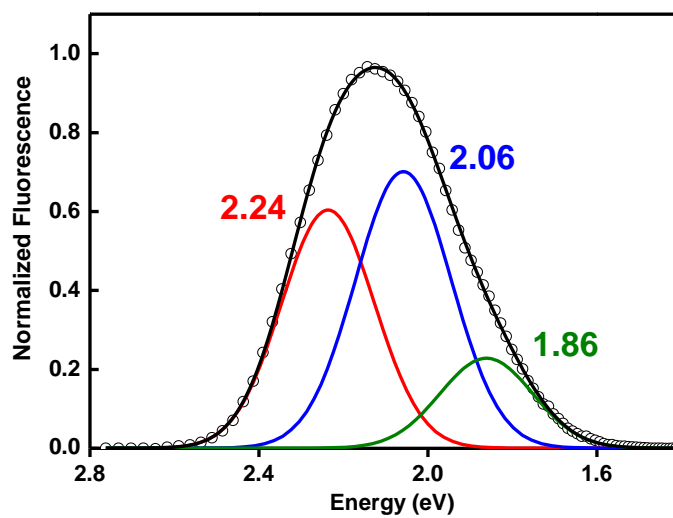


Fig. S12. PL spectra of $\frac{1}{2}$ IPT in film spin-coated on quartz substrate (open circle) and straight lines stand for Gaussian fit.

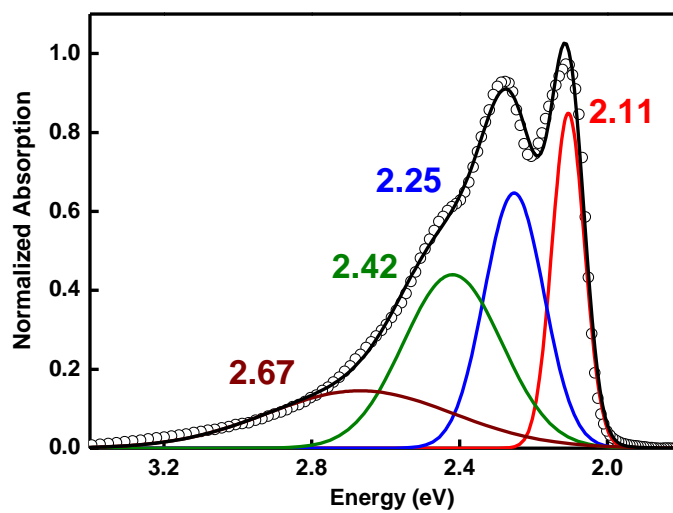


Fig. S13. UV spectra of IPT in film spin-coated on quartz substrate (open circle) and straight lines stand for Gaussian fit.

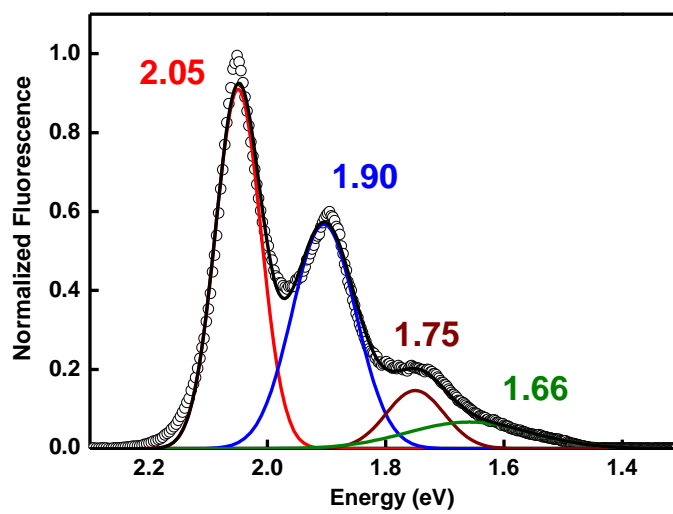


Fig. S14. PL spectra of IPT in film spin-coated on quartz substrate (open circle) and straight lines stand for Gaussian fit.

Table S1. Parameters extracted from Gaussian fits of P3HT, $\frac{1}{2}$ IPT and IPT absorption and PL.

		Peak 1		Peak 2		Peak 3		Peak 4		Peak 5		
		λ (eV)	bandwidth	λ (eV)	bandwidth	λ (eV)	bandwidth	λ (eV)	bandwidth	λ (eV)	bandwidth	
P3HT	sol	UV	2.70	0.47	3.10	0.72						
		PL	1.82	0.15	1.98	0.18	2.16	0.2				
	film	UV	2.04	0.12	2.19	0.21	2.36	0.32	2.55	0.5	2.97	0.79
		PL	1.54	0.10	1.72	0.20	1.77	0.16	1.88	0.14		
$\frac{1}{2}$ IPT	sol	UV	2.56	0.25	2.74	0.34	2.94	0.58				
		PL	1.92	0.24	2.03	0.13	2.19	0.21				
	film	UV	2.57	0.33	2.80	0.33	2.97	0.58				
		PL	1.86	0.26	2.06	0.27	2.24	0.26				
IPT	sol	UV	2.16	0.11	2.29	0.21	2.45	0.30	2.69	0.51		
		PL	1.76	0.10	1.93	0.14	2.07	0.10				
	film	UV	2.11	0.10	2.25	0.19	2.42	0.31	2.67	0.59		
		PL	1.66	0.25	1.75	0.12	1.90	0.13	2.05	0.10		

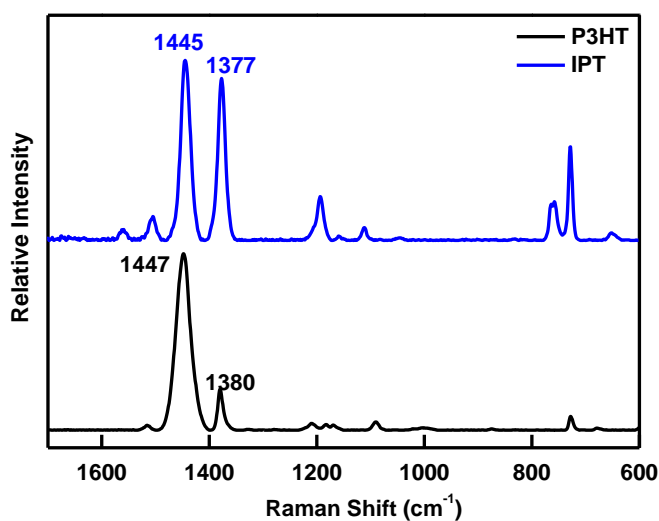
**Fig. S15.** Raman spectra of P3HT (black) and IPT (blue) in film spin-coated on quartz substrate under 532 nm excitation.

Table S2. Summary of modes of vibrations in P3HT and IPT thin films at 532 nm excitation.

	C=C symmetric stretch motion (cm ⁻¹)	C-C intraring stretch motion (cm ⁻¹)	I _{c-c} /I _{c=c}
P3HT	1448	1380	0.23
IPT	1445	1377	0.89

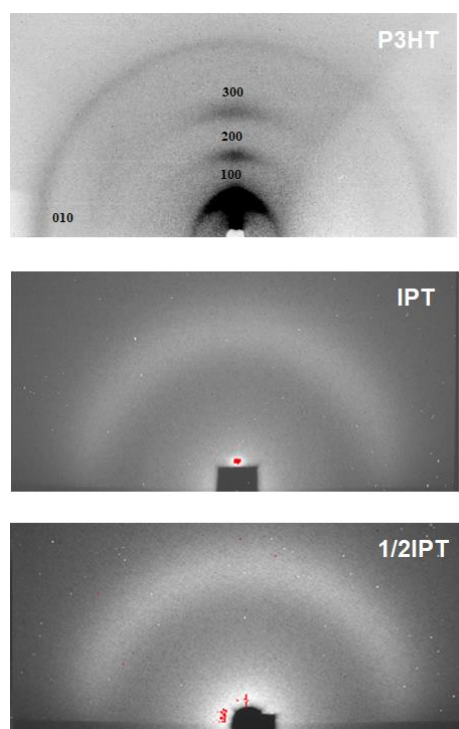


Fig. S16. GIWAXS patterns of P3HT (top) IPT, (centre) and 1/2IPT (bottom). Concerning P3HT, the (100), (200) and (300) peaks are harmonics arising from the same scattering centre. The (100) is located at $q=3.81 \text{ nm}^{-1}$ corresponding to $d=1.65 \text{ nm}$ distances, ascribed to lamellar stacking. The (010) feature at $q=15.98 \text{ nm}^{-1}$ ($d = 0.39 \text{ nm}$) is related to aromatic π - π stacking.

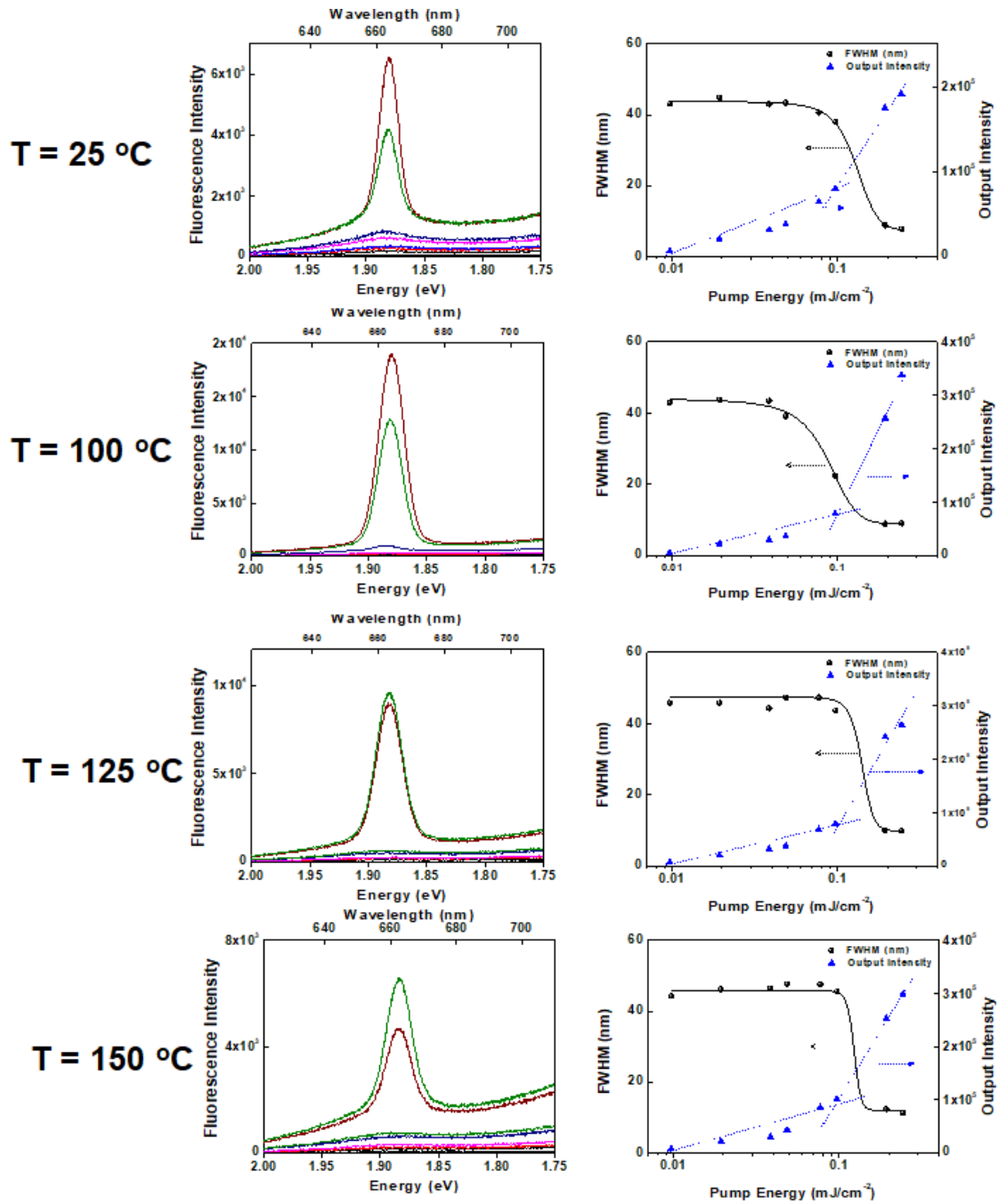


Fig. S17. ASE spectra at different pump fluences (left) and input vs. output and FWHM at different pump fluences (right) at 25°C, 100 °C, 125 °C and 150 °C.

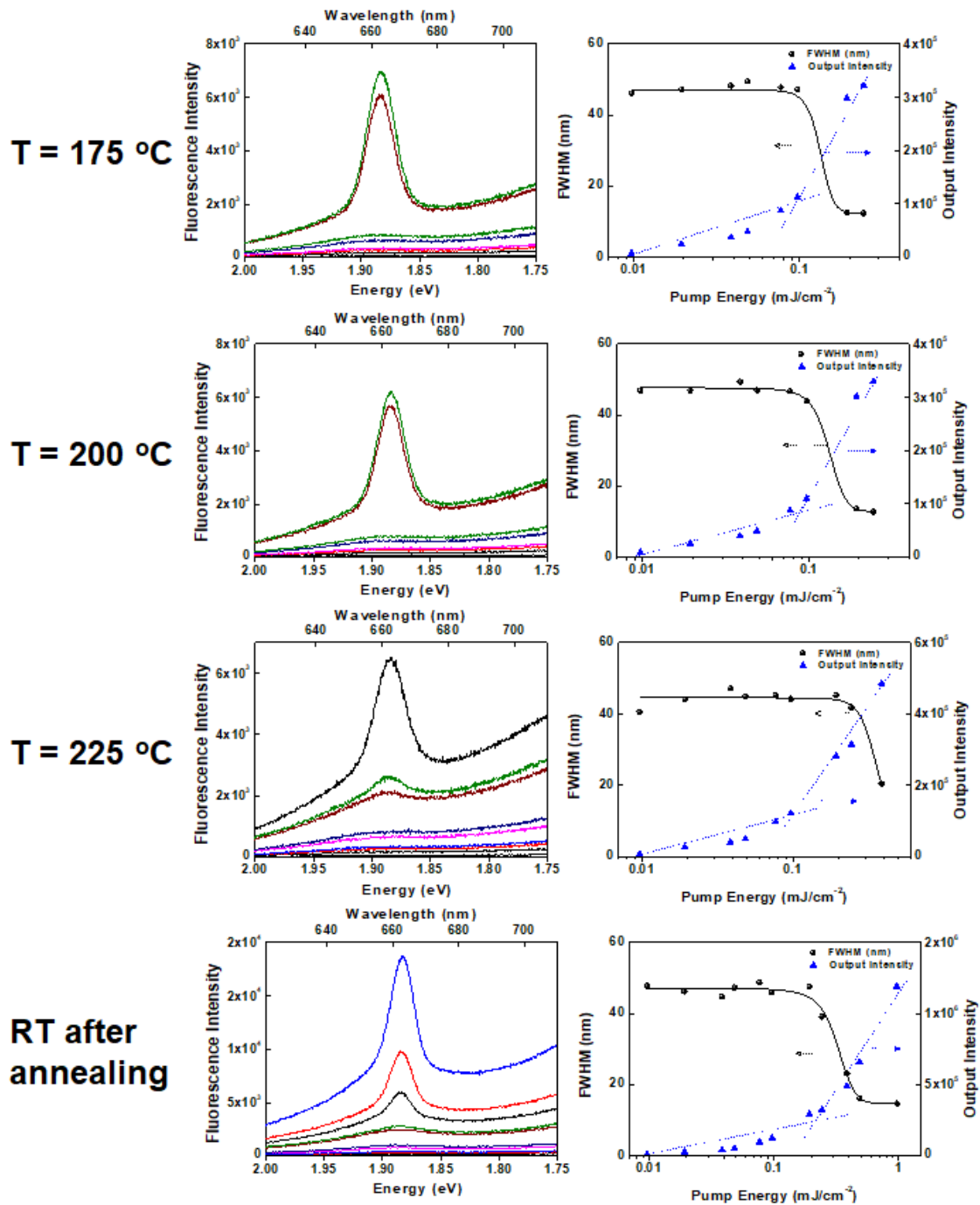


Fig. S18. ASE spectra at different pump fluences (left) and input vs. output and FWHM at different pump fluences (right) at $175\text{ }^{\circ}\text{C}$, $200\text{ }^{\circ}\text{C}$, $225\text{ }^{\circ}\text{C}$ and RT after annealing.

Table S3. ASE thresholds values of IPT as a function of temperature. ASE measurements were performed by placing an IPT film inside a cryostat with temperature controller. After reaching the desired temperature the sample was left to thermalize for about 10 minutes. Measurements were carried out in vacuum.

	25 °C	100 °C	125 °C	150 °C	175 °C	200 °C	225 °C	RT after anneal
λ_{ASE} (nm)	661	661	660	660	660	660	660	660
FWHM (nm)	7.8	9.1	9.9	11.4	12.4	12.8	20.6	14.8
$E_{\text{th}}^{\text{ASE}}$ (mJ/cm ²)	0.137	0.098	0.146	0.127	0.142	0.143	0.371	0.378

Reference

(S1) K. Sugiyasu, Y. Honsho, R. M. Harrison, A. Sato, T. Yasuda, S. Seki, and M. Takeuchi, *Journal of the American Chemical Society*, 2010, **132**, 14754-14756.